International Immunopharmacology 89 (2020) 107008

Contents lists available at ScienceDirect

International Immunopharmacology

journal homepage: www.elsevier.com/locate/intimp

IBI112, a selective anti-IL23p19 monoclonal antibody, displays high efficacy in IL-23-induced psoriasiform dermatitis

Li Li[1], Zhihai Wu[1], Min Wu[1], Xuan Qiu, Yue Wu, Zhihui Kuang, Li Wang, Ta Sun, Yang Liu, Shuai Yi, Hua Jing, Shuaixiang Zhou, Bingliang Chen, Dongdong Wu, Weiwei Wu[2,*], Junjian Liu[2,*]

Innovent Biologics (Suzhou) Co., Ltd, 168 Dongping Street, Suzhou Industrial Park, Suzhou 215123, Jiangsu, China

ARTICLE INFO

Keywords:
IBI112
IL23p19
IL-17
Half-life extension
Psoriasis

ABSTRACT

Psoriasis is a highly prevalent inflammatory skin disease. Plaque psoriasis is the most common type of psoriasis, and the interleukin (IL)-23/IL-17 axis plays a key role in disease progression. In this article, we describe IBI112, a highly potent anti-IL-23 monoclonal antibody under clinical development, which efficiently neutralizes IL23p19, a subunit of IL-23, to abrogate IL-23 binding to its receptor and block downstream signal transducer and activator of transcription 3 (STAT3) phosphorylation. Specifically, IBI112 blocked IL-23 induced downstream IL-17 production from splenocytes. In addition, IBI112 administration reduced skin thickness in a psoriasis-like epidermal hyperplasia mouse model challenged by continuous hIL-23 injection. IBI112 showed synergism with an anti-IL-1R antibody in controlling disease progression in an imiquimod (IMQ) -induced psoriasis model. Moreover, with mutations in Fc fragment of IBI112, extended half-life was observed when compared to the wild-type IgG1 version in both human-FcRn-knock-in mice and cynomolgus monkeys. IBI112 was well tolerated after high dose administration in cynomolgus monkeys. In summary, we have developed an extended half-life, anti-IL-23p19 monoclonal antibody, IBI112, which efficiently neutralized IL-23, blocked IL-23-induced IL-17 production, and alleviated disease symptoms in two mouse models of psoriasis.

1. Introduction

Autoinflammatory disease comprises a large category of immunodysfunctional disorders. Psoriasis is a highly prevalent autoinflammatory disease of the skin that affects 2% of the world's population [1,2]. Psoriasis has several subtypes, the most common one being plaque psoriasis, occurring in 85–90% of psoriasis patients and presenting as red plaques of skin covered with thick, silvery scales. Plaque psoriasis is caused by hyperproliferated, immature keratinocytes and the accumulation of neutrophils to form Munro's microabscesses. Less than half (18–42%) of psoriasis patients also develop psoriatic arthritis [3]. However, the etiology of psoriasis is not well understood, and it is not clear whether an epithelial barrier defect or abnormal immunity initiates the disease. A genome-wide association study indicated that highly susceptible loci of psoriasis are linked with both the epithelial barrier (keratinocytes) [4] and immunity (interleukin (IL)23A, IL23R, IL12B) [5]. Proinflammatory cytokines are involved in the pathogenesis of psoriasis, with IL-17 and IL-22 playing critical roles in the progression of the disease [6]. IL-17 induces keratinocytes to produce antimicrobial peptides and chemokines, which recruit a large number of neutrophils to the skin [7,8]. Neutrophils release myeloperoxidase, elastase, and reactive oxygen species, all of which cause tissue damage [9,10]. Neutrophils also disintegrate and release neutrophil extracellular traps, which comprise webs of fibers composed of chromatin and serine proteases. All of these events aggravate cutaneous inflammation [11]. IL-22 stimulates keratinocytes to proliferate, causing epidermal hyperplasia [12]. Both IL-17 and IL-22 are produced by Th17 cells. IL-23 is the key regulator that controls the proliferation and function of Th17 pathogenic cells. Although IL-6 and transforming growth factor beta (TGF-β) induce Th17 differentiation, IL-23 is required for the maturation of these cells. High levels of IL-23 have been found in lesional psoriatic skin [13]. As IL-23 controls the expression of both IL-17 [14,15] and IL-22 [16], abrogation of IL-23 dramatically reduces IL-17 and IL-22 levels [17]. IL-23 also promotes psoriatic

* Corresponding authors.
E-mail addresses: weiwei.wu@innoventbio.com (W. Wu), junjian.liu@innoventbio.com (J. Liu).
[1] These authors contributed equally to this work.
[2] These authors jointly supervised this work.

https://doi.org/10.1016/j.intimp.2020.107008
Received 11 August 2020; Received in revised form 6 September 2020; Accepted 11 September 2020

arthritis by activating osteoclast by activation of the 12-kDa-DNAX-activating protein and upregulates osteoclast-associated genes [18]. Therefore, compared to IL-17, IL-23 may be a better drug target for treating psoriasis. In addition, because of its role in inflammatory bowel disease [19,20], ankylosing spondylitis [21], and inflammatory arthritis [22,23], IL-23 inhibitors may have wider indications in many autoinflammatory diseases.

IL-23 is composed of two subunits: IL23p19 and IL12p40. The IL12p40 subunit is shared with IL-12, which is composed of IL12p40 and IL12p35. To avoid interference with IL-12 function, monoclonal antibodies have been developed to specifically target IL23p19, but not the IL12p40 subunit. Currently, three IL23p19 antibodies have been approved by the United States-Food and Drug Administration for treating psoriasis: guselkumab, risankizumab, and tildrakizumab. Guselkumab has been on the market for the longest time and has high therapeutic efficacy and a wide therapeutic window in clinical trials. Therefore, in this study, guselkumab was chosen as the benchmark antibody in some experiments. The objective of this study was to develop a humanized anti-IL23p19 antibody with extended half-life to treat psoriasis.

2. Results

2.1. IBI112 displayed high affinity for hIL-23 and impeded hIL-23 binding to hIL-23R

An anti-IL23p19 monoclonal antibody (mAb) was developed by using hybridoma technology. Briefly, Balb/c mice were immunized with a recombinant mouse IL12p40/human IL23p19 complex. Finally, clone 17D1 was selected for its highest binding affinity to the hIL-23p19 subunit, but not against the human IL12p40 subunit. After the humanization of clonal 17D1, triple mutations, M252Y/S254T/T256E (YTE), were introduced to the hIgG1 Fc of humanized clone 17D1, then the final molecule was named IBI112. The binding affinity of IBI112 and guselkumab for hIL-23 was measured by surface plasmon resonance (SPR). The equilibrium dissociation constants (KD) of IBI112 and guselkumab were 4.806E-12M and 2.859E-12M, respectively (Fig. 1A). The binding of IBI112 and guselkumab to hIL-23 was measured by the enzyme-linked immunosorbent assay (ELISA). There was no significant difference in binding activity between IBI112 and guselkumab, the EC50 of the two molecules were 1.4632 ± 0.4667 and 1.8930 ± 0.2880 nM, respectively (Fig. 1B). In addition, similar to guselkumab, IBI112 efficiently blocked hIL-23 binding to the hIL-23 receptor, the IC50 values being 1.2533 ± 0.1986 (IBI112) and 1.4720 ± 0.2610 nM (guselkumab). This indicates that, similar to guselkumab, IBI112 potently blocks hIL-23 to its receptor (Fig. 1C).

2.2. IBI112 inhibited IL-23-induced STAT3 phosphorylation in hCD4+ T cells

IL-23 binds the IL-23 receptor expressed on CD4+ T cells and directly induces intracellular STAT3 phosphorylation [24]. To investigate whether IBI112 can reduce the STAT3 phosphorylation in CD4+ T cells, serial dilutions of IBI112 or guselkumab were mixed with IL-23 before treating the T cells. Co-treatment of hCD4+ T cells with IBI112/guselkumab blocked IL-23-induced STAT3 phosphorylation. IBI112 and guselkumab had similar blocking activity with IC50 values of 87.6133 ± 21.8996 and 102.1100 ± 2.0053 nM, respectively (Fig. 2A).

2.3. IBI112 blocked IL-23-induced IL-17 production from splenocytes

Next, we determined whether IBI112 could reduce IL-17 production downstream of IL-23 signaling [25]. Serial dilutions of IBI112/guselkumab and hIL-23 were premixed and added to cultured mouse splenocytes in vitro. The concentration of mIL-17a was measured to evaluate the efficiency of IBI112 blockade. IBI112/guselkumab blocked hIL-23-induced mIL-17 production in a dose-dependent manner (IC50: IBI112: 3.8763 ± 1.0526 nM, guseklumab: 4.9743 ± 1.2847 nM) (Fig. 2B). In another experiment, we confirmed that IBI112/guselkumab also blocked IL-17F production in cynomolgus monkeys to a similar extent: IC50: IBI112:12.1950 ± 6.6680 nM, guselkumab: 16.7950 ± 5.4518 nM (Fig. 2C).

2.4. IBI112 blocked IL-23 signaling to reduce ear swelling, epidermal thickness, and inflammation

A mouse model with hIL-23-induced ear skin psoriasiform inflammation was used to test the therapeutic efficiency of IBI112. Mice were pretreated with 1 mg/kg IBI112 i.p. one day before IL-23 administration. After that, 1 μg of IL-23 was injected s.c. into the mouse ears every day for 8 days (Fig. 3A). IL-23 treatment induced ear swelling and epidermal thickness, which were significantly reduced by IBI112 (Fig. 3B, C).

In addition, IL-23 increased infiltration of inflammatory cells. Intracorneal Munro's microabcess is a unique pathology of psoriasis. IBI112 significantly reduced the number of inflammatory cells in skin. Additionally, we found that microabscesses in the stratum corneum had completely regressed after the administration of IBI112 (Fig. 3D).

2.5. IBI112 synergized with anti-IL-1R antibody in an imiquimod (IMQ)-induced skin model

As both IL-1b and IL-23 can trigger IL-17 signals that contribute to psoriasis, we investigated whether blocking both IL-23 and IL-1R pathways would reduce the severity of psoriasis in an IMQ-induced model. Details of the establishment of the animal model and dose arrangement are shown in Supplemental Fig. 1A. Disease-free survival was prolonged, and better scores were observed in the combination group of IBI112 and anti-IL-1R antibody, especially in early stage of IMQ-induced skin model, which demonstrated their synergistic effects (Supplemental Fig. 1B). Skin hematoxylin and eosin staining results confirmed this observation (Supplemental Fig. 1C). Gradual decrease of skin inflammation was observed in late stage of all groups in the IMQ-induced skin model, as has previously been described [26,27].

2.6. Better pharmacokinetic (PK) profiles of IBI112 in human FcRn-knock-in (hFcRn KI) mice

Multiple injection is needed for autoimmune patients. To improve patient compliance in clinical practice, the half-lives of Fc mutants (M252Y, S254T, T256E) of IBI112 were examined. The PK profiles of IBI112 and IBI112 with wild-type Fc were investigated in hFcRn KI mice. The half-life of IBI112 increased by ~33%, from 147 h to 196 h, when compared with the IBI112 WT Fc version. The AUC was also elevated from 15751 μg/mL*h to 21108 μg/mL*h (Fig. 4A-B). Our findings were consistent with previous findings [28] that antibodies with mutations in Fc had longer half-lives due to their higher affinity for hFcRn at pH 6.0 (Fig. 4C). Similar affinity to hFcRn was observed between IBI112 and IBI112 WT Fc version at pH 7.4 (Fig. 4D). Shorter half-lives were observed when we performed the PK comparison in wild-type mice (Supplemental Fig. 2A-B) because of higher affinity for mFcRn at pH 7.4 (Supplemental Fig. 2C). Strong binding at pH 7.4 may have a negative effect on plasma recycling and circulation persistence [29].

2.7. IBI112 showed a good safety profile in an in vitro PBMC-based system and in cynomolgus monkeys

IBI112, guselkumab, human CD3ε + CD28 (positive control), and PBS (negative control) were incubated with human peripheral blood mononuclear cells (PBMCs) for 4 and 24 h. Compared with guselkumab

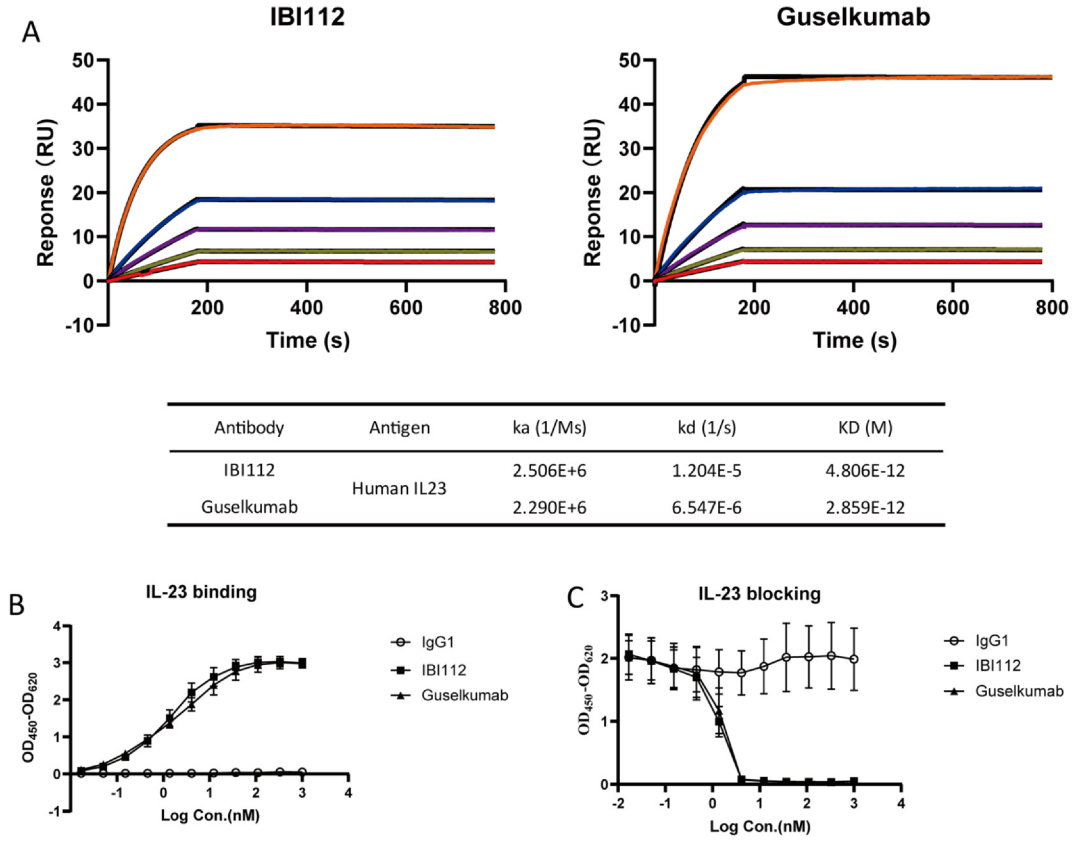

Antibody	Antigen	ka (1/Ms)	kd (1/s)	KD (M)
IBI112	Human IL23	2.506E+6	1.204E-5	4.806E-12
Guselkumab		2.290E+6	6.547E-6	2.859E-12

Fig. 1. IBI112 showed great affinity to human IL-23 and blocking capacity A, Binding affinity of IBI112 and guselkumab was measured by surface plasmon resonance (SPR) using Biacore T200. Serial dilution of human IL-23 bound with and dissociated from the antibody. B, The binding of IBI112 and guselkumab to human IL-23 was measured by ELISA. C, The blocking activity of IBI112 and guselkumab toward IL-23 was measured by ELISA. IgG1 was used as control in binding assay and blocking assay.

and human CD3ε + CD28, IBI112 did not induce significant increase of cytokines release in the tested cytokine panel including IL-6, IL-8, and TNF-α (Fig. 5A and Supplemental Table 1).

Next, we investigated the toxicological characteristics of IBI112 in single-dose and 4-week repeat-dose experiments in cynomolgus monkeys (Supplemental Table 2). In the single-dose study, 0, 50, and 100 mg/kg of IBI112 were administered subcutaneously. No test-antibody-related or toxicologically significant findings were observed after

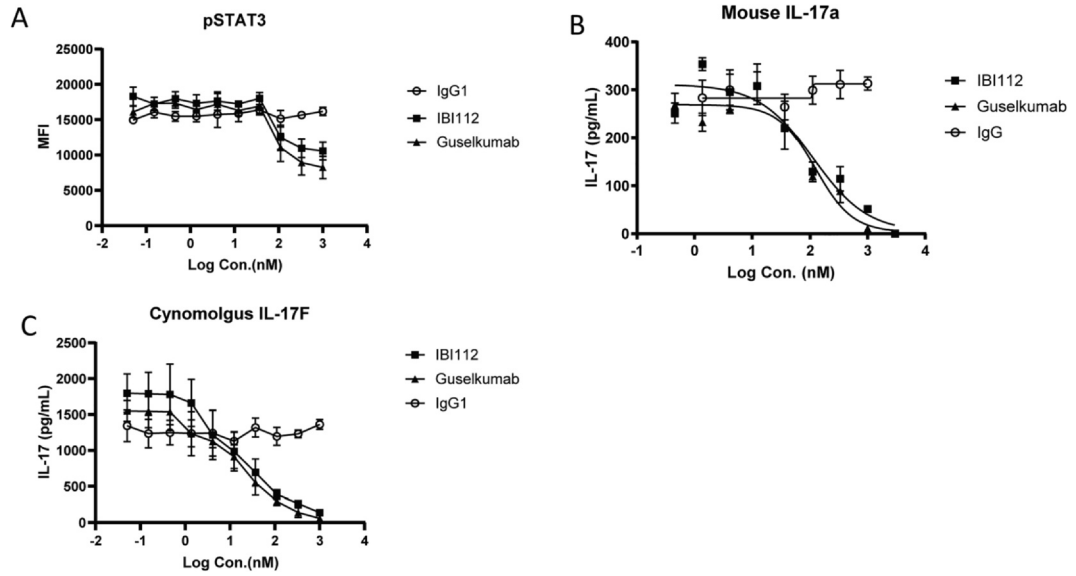

Fig. 2. IBI112 inhibited IL-23-induced IL-17 production in mouse splenocytes A, IBI112 and guselkumab inhibited IL-23-mediated STAT3 phosphorylation in human CD4 T cells, which was measured as MFI using phosphoflow staining. B-C, Serial dilutions of IBI112/guselkumab were mixed with 60 ng/mL of human IL-23. Mouse/cynomolgus monkey splenocytes were treated with the mixture for 90 h. B, Mouse IL-17 and C, cynomolgus monkey IL-17F production was measured by ELISA. IgG1 was used as control.

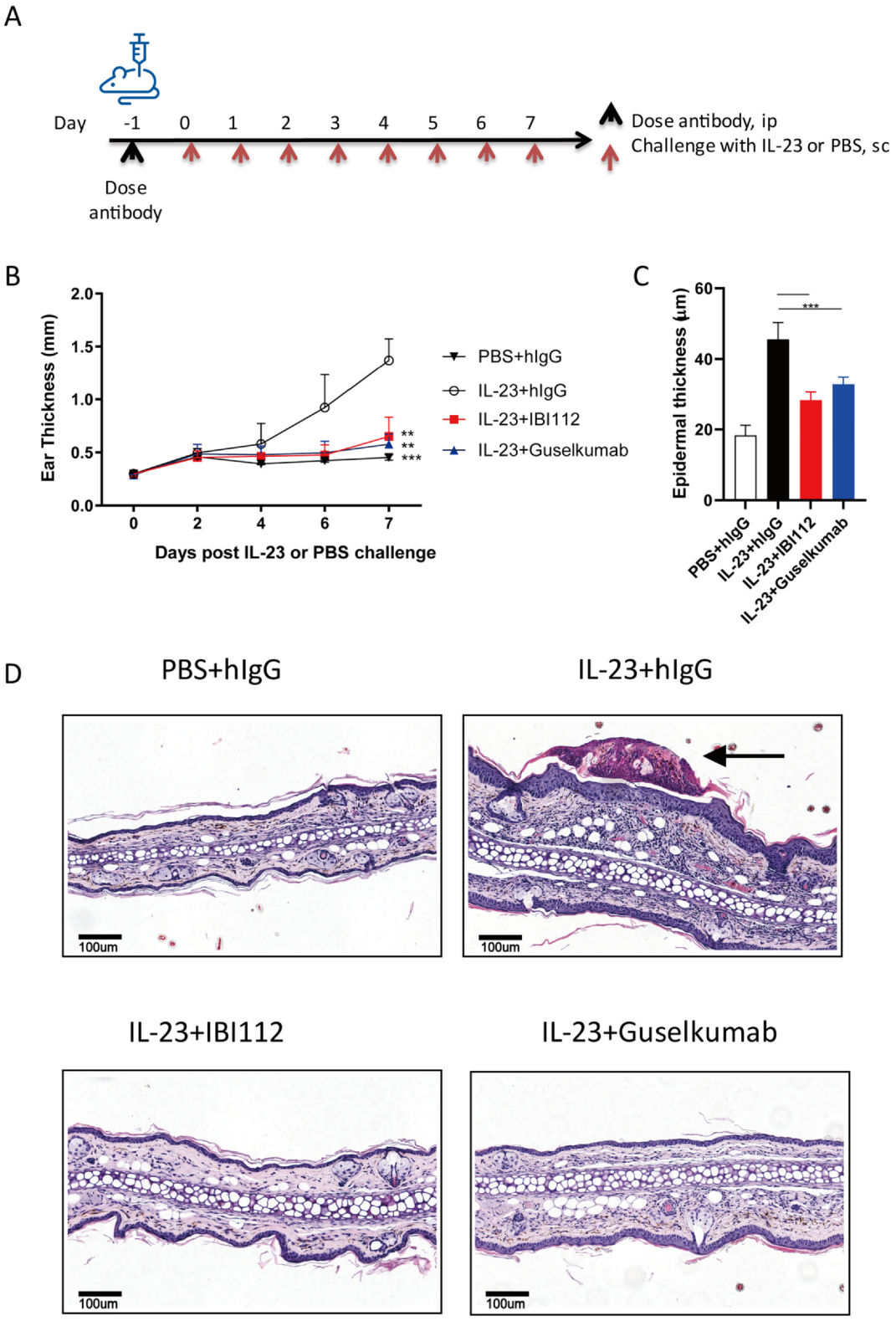

Fig. 3. IBI112 reduced hIL-23-induced mouse ear thickness and inflammation A, Anti-IL-23 antibodes were administered to mice by i.p. route on day −1. IL-23 was administered every day for 8 days by intradermal injection. For the phosphate buffered saline (PBS) group, hIgG was i.p. injected on day −1 and PBS was intradermal injection. For the hIgG group, hIgG was i.p. injected on day-1 and IL-23 was intradermal injection. B. Mouse ear swelling was measured using a caliper. C, Mouse ear epidermal thickness was calculated using Halo 2.1 software. D, Mouse ear sections were stained with hematoxylin and eosin. Black arrow: intracorneal Munro's microabscess.

A

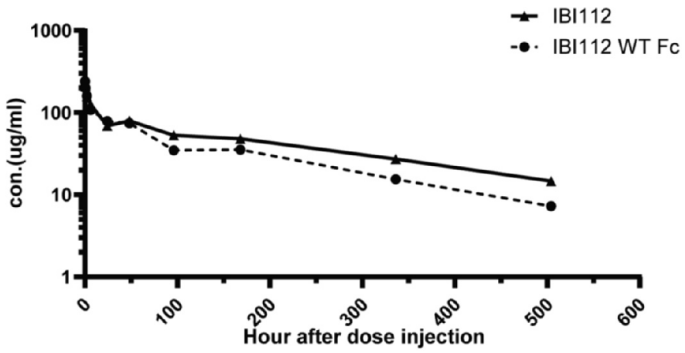

B

Group	$t_{1/2}$	C_{max}	AUC_{0-504}	Cl
	d	μg/mL	μg/mL*d	mL/d*kg
IBI112	196.56	242.48	21107.96	0.40
IBI112 WT Fc	147.32	240.46	15751.13	0.58

C

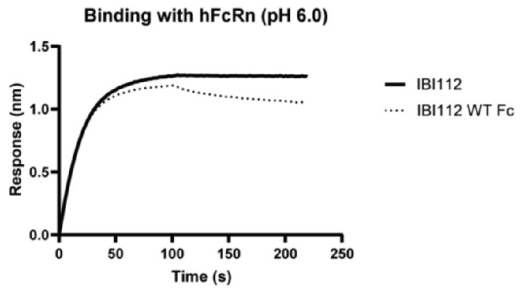

Sample ID	Response	KD (M)	kon(1/Ms)	kdis(1/s)
IBI112	1.2436	1.43E-10	4.78E+05	6.82E-05
IBI112 WT Fc	1.1651	2.82E-09	5.07E+05	1.43E-03

D

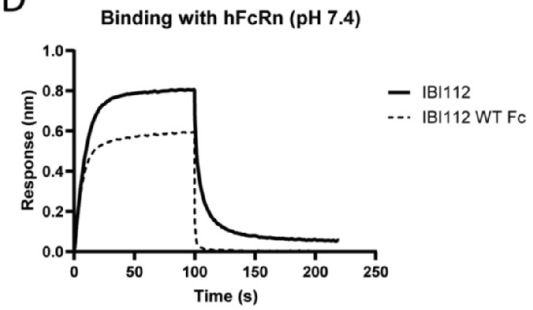

Sample ID	Response	KD (M)	kon(1/Ms)	kdis(1/s)
IBI112	0.8042	6.86E-06	1.75E+04	1.20E-01
IBI112 WT Fc	0.593	7.77E-06	3.58E+04	2.78E-01

Fig. 4. Pharmacokinetics of IBI112 in human FcRn knock-in mice and affinity of IBI112 to human FcRn. Human FcRn knock-in mice were intravenously injected with IBI112, and serum was collected for pharmacokinetic (PK) analysis. A, The PK curve was graphed using Prism Graphpad software and B, the PK parameters were calculated using the Excel plugin, PK solver 2. Compared with IBI112 WT Fc, IBI112 showed C, increased binding affinity to human FcRn at pH 6.0 and D, weak binding affinity at pH 7.4. Binding affinity were measured by biolayer interferometry (BLI) technology using Fortebio Octet Red96 and data were calculated using Data Analysis software and a 1:1 binding model (version 7.0).

14 days of observation. The maximum tolerated dose was 100 mg/kg. In the 4-week repeat-dose experiments, cynomolgus monkeys (5/sex/group) were treated subcutaneously with IBI112 at 0, 1, 10, and 50 mg/kg for 4-weeks (total of 5 doses), followed by a 4-week recovery phase. There were no unscheduled deaths, test-antibody-related, or toxicologically significant findings. The no-observed-adverse-effect-level was 50 mg/kg.

2.8. PK profile of IBI112 compared to IBI112 with wild-type Fc (IBI112-WT Fc)

The PK parameters of IBI112 were evaluated in cynomolgus monkeys. Cynomolgus monkeys were treated subcutaneously with a single dose of 1 mg/kg of IBI112 or IBI112-WT Fc. There was no sex-related difference in exposure in any group. IBI112 demonstrated higher exposure with area under curve (AUCl) of 1756.24 μg/mL*h and slower clearance with Cl of 0.51 mL/h*kg than IBI112-WT Fc (1327.58 μg/mL*h and 0.73 mL/h*kg). The half-lives (T1/2) were 299.63 and 200.08 h for IBI112 and IBI112-WT Fc, respectively (Fig. 5B-C).

3. Discussion

In this study, IBI112, an anti-IL23p19 monoclonal antibody, was developed using hybridoma technology. We selected clones that bound to IL23p19, but not to the p40 subunit. 17D1 was selected as it had the highest binding affinity among all clones. To reduce the risk of anti-drug antibody (ADA) reaction during administration to human subjects, 17D1 was engineered to become a humanized antibody and was named IBI112 after humanization. We have shown that IBI112 bound to hIL-23 without any loss in affinity. IBI112 blocked IL-23-induced STAT3 phosphorylation and IL-17 production and reduced ear skin inflammation and thickness. This antibody demonstrated blockade efficacy comparable to that of guselkumab. There was no obvious toxicity even with a high dose of 50 mg/kg in cynomolgus monkeys. To improve patient compliance in clinical practice, a better pharmacokinetic profile IBI112 was engineered and no ADA reaction was detected.

We generated an antibody, which targets IL23p19, but not the IL12p40 subunit. This strategy avoids interference with the IL-12 pathway. IL-12 and IL-23 are heterodimeric cytokines that share the same IL12p40 subunit, and IL-12 shows great potency in anti-tumor

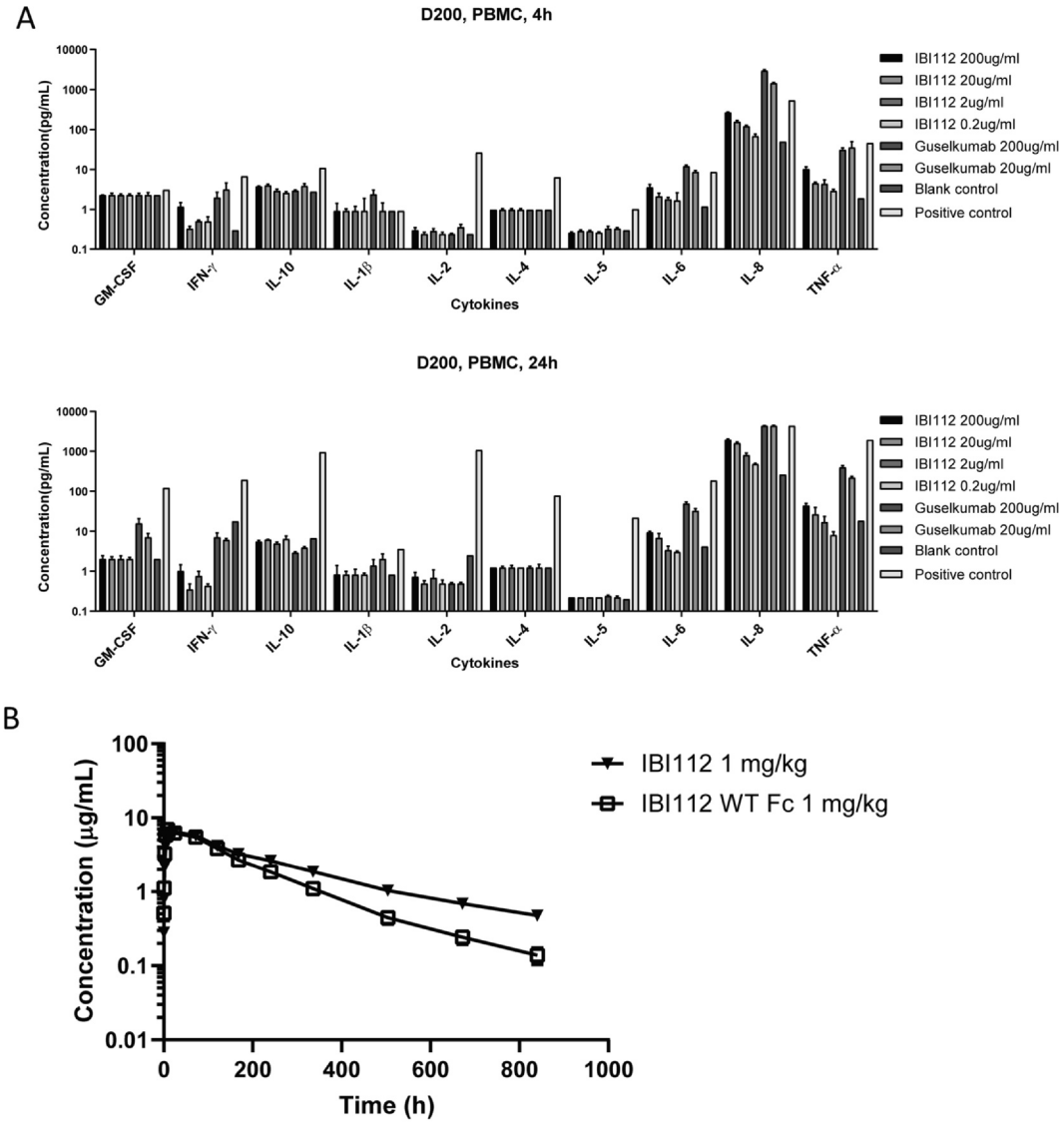

C

Group	$t_{1/2}$	C_{max}	AUC_{0-840}	Cl
	h	μg/mL	μg/mL*h	mL/h*kg
IBI112	299.63	6.45	1756.24	0.51
IBI112 WT Fc	200.08	6.92	1327.58	0.73

Fig. 5. IBI112 did not cause cytokine release from PBMCs, and pharmacokinetics of IBI112 and guselkumab in cynomolgus monkeys. A, Cytokine release assay. PBS, 20, or 200 μg/mL of mAbs, 10 μg/mL + 10 μg/mL of human CD3ε + CD28 were incubated with human PBMCs for 4 (upper panel) and 24 h (lower panel). Levels of ten cytokines were measured using Luminex. Results shown are from one donor; three independent experiments were performed on 3 different healthy donors. B, IBI112 (1 mg/kg) and guselkumab were administered subcutaneously to cynomologus monkeys. After administration, blood samples were collected at different time points. Blood serum concentrations of these drugs were measured by ELISA. C, Pharmacokinetics of IBI112 and IBI112 WT Fc.

immunotherapy [30] and confers cellular immunity to intracellular pathogens. Therefore, specifically targeting IL23p19 improves safety and avoids potential side effects.

Psoriasis is an autoinflammatory skin disease driven by multiple genes. The IL-23/IL-17 axis plays a major role in psoriasis, and IL-1 has also been implicated as a key player in the pathogenesis of psoriasis. A genetic study has described IL-1R1 as a new susceptibility locus for psoriasis [31]. Levels of IL-1b and IL-1Ra are significantly elevated in human psoriatic skin [32,33]. The IL-1b pathway is critical for the development of IL17-expressing T cells, and blocking IL-1b with canakinumab has been shown to lead to complete skin clearance and eradication of symptoms after one year of continuous canakinumab therapy [34]. Our study reveals that blocking of both the IL-23 and IL-1 pathways generated better outcomes in an IMQ-induced psoriasis mouse model. Greater alleviation of symptoms such as less scaling, erythema, and skin thickness were observed with the combination of IBI112 and a-IL-1R, suggesting a potential combination strategy for clinical use.

Psoriasis is a widespread and chronic disease with no cure. Psoriasis patients need continuous, long-term treatment with 6–34 injections in

the first year and at least 4 injections in the following years [35–40]. Our study aimed at developing an antibody with an extended half-life to reduce the frequency of injections. The triple mutation, M252Y/S254T/T256E (YTE), which increases the affinity to human FcRn at pH 6.0, was introduced into the Fc portion of IBI112 to extend its half-life. The half-life extension was demonstrated in hFcRn KI mice and cynomolgus monkeys in this study and in another study as well [41]. In summary, IBI112 is a promising drug candidate that can provide better clinical outcomes for the treatment of psoriasis.

4. Materials and methods

4.1. Generation of hIL23p19 antibodies and screening

To select hIL23p19 antibodies, BALB/c mice (Beijing Vital River Laboratory, China) were immunized with a recombinant mouse IL-23p40/human IL23p19 hybrid molecule. Hybridomas were generated by standard cell fusion method using mouse myeloma SP2/0 cells. Antibody binders were selected by ELISA for their ability to only interact with human IL23p19, but not with human IL12p40. Next, the selected binders were screened for their blocking activity in an IL-17 production inhibition assay.

The IL-23 binding ELISA assay was performed in 96-well ELISA plates coated with IL-23 at 1 μg/mL in carbonate buffer, 4 °C, overnight. After blocking with 200 μL ELISA assay diluents with 5% bovine serum albumin (BSA). 100 μL of hybridoma supernatants or diluted purified mAbs were added and incubated for 1 h. After incubation and washing, horseradish peroxidase (HRP) -labeled anti-human secondary IgG Fc antibody (Ab) was added. The plate was developed using TMB (SolarBio, China), and the readings were measured by using an ELISA plate reader (Molecular Device, USA). All functional antibodies used in the study were purifed in-house (Innovent Biologics Co., Ltd., Suzhou, China) with HEK293 cells by either transient or stable expression.

4.2. IL-23 binding assay

Recombinant IL-23 (R&D, USA, 1 μg/mL) was used to coat plates overnight. A coated plate was washed, and different concentrations of IBI112/guselkumab were added to the plate. After incubation and washing, HRP-labeled anti-human secondary IgG Fc antibody (Ab) was added. The plate was developed using TMB (3,3′,5,5′-Tetramethylbenzidine, SolarBio, China), and the readings were measured by using an ELISA plate reader (Molecular Device, USA).

4.3. Inhibition of IL-17 production

Mouse (C57BL/6, Beijing Vital River Laboratory Animal Technology) or cynomolgus monkey splenocytes (AllCells, USA) were cultured in the presence of IL-2 (R&D, USA). Different concentrations of antibodies or supernatants of hybridoma clones were mixed with 60 ng/mL of IL-23. The mixture was added to cultured mouse/cynomolgus monkey splenocytes and incubated for 90 h. After incubation, the supernatants were collected to measure the IL-17 concentration by using a mouse/cynomolgus monkey IL-17 DuoSet ELISA kit (R&D Systems, USA).

4.4. Receptor blocking assay

IL-23R solution (1 μg/mL) was used to coat plates overnight. A coated plate was washed with 0.05% PBST and blocked with 2% BSA-PBST. IL-23-biotin (R&D, USA) was added to the medium, and different concentrations of IBI112/guselkumab and 1 μg/mL of rhIL-23-Biotin were mixed and added to the plate. IL-23 binding to IL-23R was measured by ELISA.

4.5. SPR detection

The binding affinity of IBI112 and human IL-23 was measured with a Biacore T200 (GE Healthcare, USA). Briefly, IBI112 was captured and fixed on a pro A chip (GE Healthcare). Different concentrations of human IL-23 (0, 0.2, 0.4, 0.8, 1.6, 3.2, 6.4 nM) (R&D systems, USA) were added for binding to and dissociation from the antibody. The binding time was 180 s, and the dissociation time was 600 s. Dilutions and experiments were performed at 25 °C in HBS-EP+ buffer (GE Healthcare, USA). All data were analyzed using Biacore analysis software (Version 3.1) and a 1:1 binding model.

4.6. FcRn binding affinity by biolayer interferometry (BLI)

Affinity to human and mouse FcRn for IBI112 at both pH 6.0 and pH 7.4 was tested using BLI technology and an Octet Red 96 (Fortebio, USA). Biotinylated human FcRn (Acro Biosystems, USA) and mouse FcRn (Acro Biosystems, USA) were first immobilized onto SA biosensors (Fortebio, USA) at a level of ~0.5 nm. The biosensors were subsequently dipped into a 100 nM IBI112 solution with an association time of 100 s, followed by dissociation for 120 s in running buffer (PBS with 0.1% BSA and 0.05% tween 20) at room temperature. The binding affinity data were fitted using Data Analysis software (Version 7.0) and a 1:1 binding model.

4.7. STAT3 phosphorylation

Human CD4+ T cells were purified from human PBMCs (AllCells, USA) by using an Easysep human CD4 T cell enrichment kit (Stemcell Technologies, Canada). CD4+ T cells were cultured in the presence of Dynabeads Human T-Activator CD3/CD28 (Invitrogen, USA) for 7 days: 50 ng/mL of hTGF-β (Acro Biosystems, USA) and 10 ng/mL of hIL-6 (R&D) were added over the first 3 days, and from day 4 onwards, the cytokines were replaced with 5 ng/mL of hIL-1β and 10 ng/mL of hTNF-α for another 4 days. Polarized CD4+ T cells were subsequently harvested. Serial dilutions of IBI112 or guselkumab were mixed with 4 μg/mL of hIL-23, and the mixture was incubated with the polarized T cell culture for 40 min. The T cells were fixed, permeabilized, and stained with PE-conjugated, phospho-STAT3 Ab (BioLegend, USA). The MFI of phospho-STAT3 was measured by flow cytometry (BD Biosciences, USA).

4.8. Ear skin swelling and epidermal thickness measurement

We used 6–8-week-old female C57BL/6 mice (Beijing Vital River Laboratory Animal Technology, N = 5 for PBS + hIgG group, N = 6 for other groups) to test the in vivo efficacy of IBI112. All animals were maintained under pathogen-free conditions in the Experimental Animal Center of Innovent Biologics Co., Ltd. (Suzhou, China). All animal-related experiments were approved by the Animal Use and Care Committee of Innovent Biologics. One day before IL-23 administration, 1 mg/kg IBI112 or hIgG was injected intraperitoneally, whereas 1 μg of hIL-23 (R&D) or PBS was injected subcutaneously into the ear every day for 8 days. Mouse ear skin thickness was measured using a caliper on days 1, 3, 5, and 7. After day 7, mouse ears were harvested, fixed, embedded in paraffin, and stained with hematoxylin and eosin. The epidermal thickness was measured by using HALO 2.1 Tissue Classifier software (Indica Labs, USA).

4.9. IMQ-induced psoriasis model

An IMQ-induced psoriasis-like mouse model was established as described previously [32]. Briefly, IMQ cream (Sinopharm, China) was applied every day on the shaved back of human IL-23-knock-in female mice (Shanghai Model Organisms Center, N = 1 for the normal group, N = 5 for other groups) for 5 consecutive days from day 0 onwards.

IBI112 and anti-IL-1R antibody (Bioxcell, BE0256) were administered at day 0 and day 3. Scaling erythema and skin thickness were calculated according to the psoriasis area severity index. All mice were housed and bred in specific pathogen–free conditions in the Animal Barrier Facility at the Shanghai Model Organisms Center (SMOC). All mouse experiments were approved by the Institutional Animal Care and Use Committee of SMOC.

4.10. IBI112 toxicology analysis in cynomolgus monkeys

Cynomolgus monkeys were provided by WestChina-Frontier PharmaTech, Sichuan, China. All monkey experiments were approved by the Institutional Animal Care and Use Committee of WestChina-Frontier PharmaTech. All monkey studies were performed by WestChina-Frontier PharmaTech. Both single dosing and 4-week dosing were performed.

For single-dose toxicology experiments, 9 cynomolgus monkeys (3/group, including males and females) were treated subcutaneously with 0, 50 mg/kg and 100 mg/kg IBI112, respectively. The monkeys were kept for observation for 14 days during and after which a variety of physiological parameters were measured. These included body weight, complete blood counts and chemistry, blood pressure, food intake, electrocardiogram (ECG), urine, immune cell subpopulations, immunoglobulin, complement (C3, C4), circulating immune complex (CIC), troponin T and gross necropsy macrohistology. The TK and ADA was also detected.

For multiple dosing toxicology experiments, 4 groups (5/sex/group) of cynomolgus monkeys were subcutaneously treated with 0, 1, 10, and 50 mg/kg IBI112 every week for 4 weeks (totally 5 times). The monkeys were kept for recovery for ~4 weeks after treatment. During the periods of dosing and recovery, the same physiological parameters were measured as those mentioned for single-dose experiments.

4.11. Cytokine release assay for PBMCs

For the cytokine release assay, plate-bound IBI112 (20, 200 μg/mL), guselkumab (20, 200 μg/mL), human CD3ε + CD28 (10 μg/mL + 10 μg/mL, positive control), and PBS (negative control) were incubated with human PBMCs for 4 and 24 h, respectively. Concentrations of IFN-γ, TNF-α, IL-1β, IL-2, IL-4, IL-6, IL-10, IL-8, IL-5, and GM-CSF in the PBMC supernatants were measured by using the Luminex assay (Thermo Fisher, USA). The cytokine release assay was performed by Crown Biosciences.

4.12. Pharmacokinetics of IBI112 and guselkumab in human FcRn-knock-in mice and cynomolgus monkeys

The pharmacokinetics profiles of IBI112 and IBI112 WT Fc were analyzed in hFcRn-KI (Biocytogen Co., Ltd, Beijing, N = 9 for each group) female mice as follows: 10 mg/kg antibody was injected intravenously, and blood serum was collected for further ELISA measurement. Pharmacokinetic parameters were calculated by PK solver add-in in Excel [42].

The pharmacokinetics profiles of IBI112 and IBI112 WT Fc were evaluated in cynomolgus monkeys (3 males and 3 females for each group) following subcutaneous administration of a single dose of 1 mg/kg antibody. Blood serum was collected, and serum concentrations of the mAbs were measured using hIL-23-captured ELISA. Cmax, AUCall, and T1/2 were calculated by using the PK solver add-in in Excel.

Author contributions

Li Li provided the hybridoma platform; Zhihai Wu, Yue Wu designed and performed the affinity measurement experiments; Shuaixiang Zhou, Li Wang designed and prepared all the needed protein; Zhihui Kuang, Hua Jing designed and performed the in vitro assays; Min Wu, Ta Sun, Shuai Yi, Yang Liu, Weiwei Wu, Bingliang Chen designed and performed all the in vivo mouse experiment; Xuan Qiu, Dongdong Wu performed experiments in primate; Weiwei Wu, Junjian Liu designed the study. All authors read and approved the final manuscript.

Disclosure of Potential Conflicts of Interest

All authors are employees of Innovent Biologics (Suzhou).

Appendix A. Supplementary material

Supplementary data to this article can be found online at https://doi.org/10.1016/j.intimp.2020.107008.

References

[1] S.P. Raychaudhuri, E.M. Farber, The prevalence of psoriasis in the world, J. Eur. Acad. Dermatol. Venereol. 15 (2001) 16–17, https://doi.org/10.1046/j.1468-3083.2001.00192.x.
[2] H.-Y. Chiu, et al., Psoriasis in Taiwan: From epidemiology to new treatments, Dermatol. Sinica 36 (2018) 115–123, https://doi.org/10.1016/j.dsi.2018.06.001.
[3] D.D. Gladman, C. Antoni, P. Mease, D.O. Clegg, P. Nash, Psoriatic arthritis: epidemiology, clinical features, course, and outcome, Ann. Rheum. Dis. 64 (Suppl 2) (2005) ii14-17, https://doi.org/10.1136/ard.2004.032482.
[4] D.M. Berki, et al., Activating CARD14 mutations are associated with generalized pustular psoriasis but rarely account for familial recurrence in psoriasis vulgaris, J, Invest. Dermatol. 135 (2015) 2964–2970, https://doi.org/10.1038/jid.2015.288.
[5] R.P. Nair, et al., Genome-wide scan reveals association of psoriasis with IL-23 and NF-kappaB pathways, Nat. Genet. 41 (2009) 199–204, https://doi.org/10.1038/ng.311.
[6] L.E. Durham, B.W. Kirkham, L.S. Taams, Contribution of the IL-17 pathway to psoriasis and psoriatic arthritis, Curr. Rheumatol. Rep. 17 (2015) 55, https://doi.org/10.1007/s11926-015-0529-9.
[7] S. Yu, et al., Diet-induced obesity exacerbates imiquimod-mediated psoriasiform dermatitis in anti-PD-1 antibody-treated mice: Implications for patients being treated with checkpoint inhibitors for cancer, J. Dermatol. Sci. 97 (2020) 194–200, https://doi.org/10.1016/j.jdermsci.2020.01.011.
[8] S. Yu, et al., A Western diet, but not a high-fat and low-sugar diet, predisposes mice to enhanced susceptibility to imiquimod-induced psoriasiform dermatitis, J, Invest. Dermatol. 139 (2019) 1404–1407, https://doi.org/10.1016/j.jid.2018.12.002.
[9] N. Dilek, et al., Contribution of myeloperoxidase and inducible nitric oxide synthase to pathogenesis of psoriasis, Postepy Dermatol. Alergol. 33 (2016) 435–439, https://doi.org/10.5114/ada.2016.63882.
[10] P. Rocha-Pereira, et al., The inflammatory response in mild and in severe psoriasis, Br. J. Dermatol. 150 (2004) 917–928, https://doi.org/10.1111/j.1365-2133.2004.05984.x.
[11] S.C.-S. Hu, et al., Neutrophil extracellular trap formation is increased in psoriasis and induces human β-defensin-2 production in epidermal keratinocytes, Sci. Rep. 6 (2016) 31119, https://doi.org/10.1038/srep31119.
[12] S. Pantelyushin, et al., Rorgammat + innate lymphocytes and gammadelta T cells initiate psoriasiform plaque formation in mice, J. Clin. Invest. 122 (2012) 2252–2256, https://doi.org/10.1172/JCI61862.
[13] E. Lee, et al., Increased expression of interleukin 23 p19 and p40 in lesional skin of patients with psoriasis vulgaris, J. Exp. Med. 199 (2004) 125–130, https://doi.org/10.1084/jem.20030451.
[14] D. Yen, et al., IL-23 is essential for T cell-mediated colitis and promotes inflammation via IL-17 and IL-6, J. Clin. Investig. 116 (2006) 1310–1316, https://doi.org/10.1172/JCI21404.
[15] G.X. Zhang, et al., Induction of experimental autoimmune encephalomyelitis in IL-12 receptor-beta 2-deficient mice: IL-12 responsiveness is not required in the pathogenesis of inflammatory demyelination in the central nervous system, J. Immunol. 170 (2003) 2153–2160, https://doi.org/10.4049/jimmunol.170.4.2153.
[16] L. Zhou, et al., IL-6 programs T(H)-17 cell differentiation by promoting sequential engagement of the IL-21 and IL-23 pathways, Nat. Immunol. 8 (2007) 967–974, https://doi.org/10.1038/ni1488.
[17] K.I. Happel, et al., Divergent roles of IL-23 and IL-12 in host defense against Klebsiella pneumoniae, J. Exp. Med. 202 (2005) 761–769, https://doi.org/10.1084/jem.20050193.
[18] H.S. Shin, et al., Crosstalk among IL-23 and DNAX activating protein of 12 kDa-dependent pathways promotes osteoclastogenesis, J. Immunol. 194 (2015) 316–324, https://doi.org/10.4049/jimmunol.1401013.
[19] J. Sabino, B. Verstockt, S. Vermeire, M. Ferrante, New biologics and small molecules in inflammatory bowel disease: an update, Therap. Adv. Gastroenterol. 12 (2019), https://doi.org/10.1177/1756284819853208.
[20] T.A. Gheita, G. El II, H.S. El-Fishawy, M.A. Aboul-Ezz, S.A. Kenawy, Involvement of IL-23 in enteropathic arthritis patients with inflammatory bowel disease: preliminary results, Clin. Rheumatol. 33 (2014) 713–717, https://doi.org/10.1007/s10067-013-2469-y.
[21] P. Rahman, et al., Association of interleukin-23 receptor variants with ankylosing

spondylitis, Arthritis Rheum. 58 (2008) 1020–1025, https://doi.org/10.1002/art.23389.
[22] G. Orozco, B. Rueda, G. Robledo, A. Garcia, J. Martin, Investigation of the IL23R gene in a Spanish rheumatoid arthritis cohort, Hum. Immunol. 68 (2007) 681–684, https://doi.org/10.1016/j.humimm.2007.05.008.
[23] A. Paradowska-Gorycka, A. Grzybowska-Kowalczyk, E. Wojtecka-Lukasik, S. Maslinski, IL-23 in the pathogenesis of rheumatoid arthritis, Scand. J. Immunol. 71 (2010) 134–145, https://doi.org/10.1111/j.1365-3083.2009.02361.x.
[24] M.-L. Cho, et al., STAT3 and NF-κB signal pathway is required for IL-23-mediated IL-17 production in spontaneous arthritis animal model IL-1 Receptor antagonist-deficient mice, J. Immunol. 176 (2006) 5652–5661, https://doi.org/10.4049/jimmunol.176.9.5652.
[25] S. Singh, et al., Selective targeting of the IL23 pathway: Generation and characterization of a novel high-affinity humanized anti-IL23A antibody, mAbs 7 (2015) 778–791, https://doi.org/10.1080/19420862.2015.1032491.
[26] J. Manils, et al., The Exonuclease Trex2 Shapes Psoriatic Phenotype, J, Invest. Dermatol. 136 (2016) 2345–2355, https://doi.org/10.1016/j.jid.2016.05.122.
[27] J. Palomo, S. Troccaz, D. Talabot-Ayer, E. Rodriguez, G. Palmer, The severity of imiquimod-induced mouse skin inflammation is independent of endogenous IL-38 expression, PLoS One 13 (2018) e0194667, https://doi.org/10.1371/journal.pone.0194667.
[28] W.F. Dall'Acqua, P.A. Kiener, H. Wu, Properties of human IgG1s engineered for enhanced binding to the neonatal Fc receptor (FcRn), J. Biol. Chem. 281 (2006) 23514–23524, https://doi.org/10.1074/jbc.M604292200.
[29] P.R. Cooper, et al., The contribution of cell surface FcRn in monoclonal antibody serum uptake from the intestine in suckling rat pups, Front. Pharmacol. 5 (2014) 225, https://doi.org/10.3389/fphar.2014.00225.
[30] A. Mansurov, et al., Collagen-binding IL-12 enhances tumour inflammation and drives the complete remission of established immunologically cold mouse tumours, Nat. Biomed. Eng. 4 (2020) 531–543, https://doi.org/10.1038/s41551-020-0549-2.
[31] X. Zuo, et al., Whole-exome SNP array identifies 15 new susceptibility loci for psoriasis, Nat. Commun. 6 (2015) 6793, https://doi.org/10.1038/ncomms7793.
[32] Y. Cai, et al., A critical role of the IL-1beta-IL-1R signaling pathway in skin inflammation and psoriasis pathogenesis, J. Invest. Dermatol. 139 (2019) 146–156, https://doi.org/10.1016/j.jid.2018.07.025.
[33] H.J. Kim, et al., Up-regulation of receptor antagonist interleukin-1 family members in psoriasis and their regulation by pro-inflammatory cytokines, J. Dermatol. Sci. 82 (2016) 204–206, https://doi.org/10.1016/j.jdermsci.2016.02.003.
[34] P. Skendros, et al., Successful response in a case of severe pustular psoriasis after interleukin-1beta inhibition, Br. J. Dermatol. 176 (2017) 212–215, https://doi.org/10.1111/bjd.14685.
[35] (guselkumab), T. Janssen Biotech, Inc. Drug label. https://www.accessdata.fda.gov/drugsatfda_docs/label/2017/761061s000lbl.pdf.
[36] (ixekizumab), T. Eli Lilly Company. Drug label. https://www.accessdata.fda.gov/drugsatfda_docs/label/2017/125521s004lbl.pdf.
[37] (risankizumab-rzaa), S. AbbVie Inc. Drug label. https://www.accessdata.fda.gov/drugsatfda_docs/nda/2019/761105Orig1s000Lbl.pdf.
[38] (secukinumab), C. Novartis Pharmaceuticals Corporation. Drug label. https://www.accessdata.fda.gov/drugsatfda_docs/label/2020/125504s031lbl.pdf.
[39] ILUMYA™. Merck & Co., Inc. Drug label. https://www.accessdata.fda.gov/drugsatfda_docs/label/2018/761067s000lbl.pdf.
[40] Stelara®(ustekinumab). Janssen Biotech, Inc. Drug label. https://www.accessdata.fda.gov/drugsatfda_docs/label/2016/761044lbl.pdf.
[41] G.J. Robbie, et al., A novel investigational Fc-modified humanized monoclonal antibody, motavizumab-YTE, has an extended half-life in healthy adults, Antimicrob. Agents Chemother. 57 (2013) 6147–6153, https://doi.org/10.1128/AAC.01285-13.
[42] Y. Zhang, M. Huo, J. Zhou, S. Xie, PKSolver: An add-in program for pharmacokinetic and pharmacodynamic data analysis in Microsoft Excel, Comput. Methods Programs Biomed. 99 (2010) 306–314, https://doi.org/10.1016/j.cmpb.2010.01.007.